Surface Texture of Poly(styrenesulfonate sodium salt) and Poly(diallyldimethylammonium chloride) Micron-Sized Multilayer Capsules: A Scanning Force and Confocal Microscopy Study

Changyou Gao,[†,‡,§] Stefano Leporatti,[‡,§] Edwin Donath,[*,‡] and Helmuth Möhwald[‡]

Department of Polymer, Zhejiang University, Hangzhou 310027, China, and Max-Planck Institute of Colloids and Interfaces, D-14424 Golm/Potsdam, Germany

Received: February 17, 2000; In Final Form: May 3, 2000

Ultrathin polyelectrolyte capsules fabricated by stepwise assembly of poly(styrenesulfonate sodium salt) and poly(diallyldimethylammonium chloride) are examined by confocal laser scanning microscopy and scanning force microscopy. The capsule surface is composed of grains of 124 ± 10 nm in diameter with a roughness of ∼13 nm. These grains are formed by laterally segregated polyelectrolyte complexes. Osmotically and annealing-induced capsule swelling facilitated further grain segregation together with a capsule surface area increase. Incubation in salt solution induced capsule shrinking and grain aggregation.

Introduction

A novel pathway for fabricating polyelectrolyte capsules with ultrathin multilayer walls based on the layer-by-layer adsorption technique[1−4] was developed recently.[5] Oppositely charged polyelectrolytes were consecutively adsorbed onto charged colloidal templates, followed by decomposition of the templates. The typical polyelectrolyte capsules produced so far were composed of alternating poly(stryrenesulfonate sodium salt) (PSS) and poly(allylamine hydrochloride) (PAH). These capsules were characterized with respect to their morphology, surface charge, their wall texture, layer capacitance, and conductance, and their stability upon temperature increase.[5−12]

Recently, instead of PAH, another polycation, poly(diallyldimethylammonium chloride) (PDADMAC), was employed for the preparation of PSS/PDADMAC capsules. Capsules that are impermeable for macromolecules were obtained with a yield higher than 90%. Preliminary studies revealed that PSS/PDADMAC capsules are different from PSS/PAH capsules concerning their elasticity, and their response to higher temperatures and salt addition.

It was recently shown that the PSS/PAH capsules exhibit a typical lateral texture in the submicron scale. Grains of a size of about 70 nm in diameter were observed. These grains were interpreted as segregated polyelectrolyte complexes.[9,10] The mechanism of grain formation and their significance for the capsule wall properties is at present not understood. Therefore, it is interesting to study also the texture of the new PSS/PDADMAC capsules and to compare it with PSS/PAH capsules. One may expect that changing PAH for PDADMAC may influence the layer properties and the appearance of the grains. This would promote a better understanding of the molecular mechanism of capsule formation and of the relation between molecular composition and capsule properties.

This study reports data on the nanometer scale lateral structure of PSS/PDADMAC capsules. A grainy texture of the PSS/PDADMAC capsule wall was indeed observed by SFM at high resolution. The grains were significantly larger than those reported for PSS/PAH capsules. PSS/PDADMAC multilayers deposited on mica had a similar grain size but revealed a more inhomogeneous distribution of the grains. Capsule swelling as a result of an osmotic pressure difference or heating induced a larger separation of the grains. The two cationic polymers that we can now compare differ in their stiffness, dimension of the ionic group, and charge density along the backbone and molecular weight. These features in relation to PSS are discussed in view of consequences for structure and permeability.

Materials and Methods

Materials. The sources of chemicals were as follows: PSS, M_w 70 000 and PDADMAC, medium $M_w \sim 200-350$ kDa, 20 wt % in water, Aldrich; weakly cross-linked melamine formaldehyde particles (MF-particles), microparticles GmbH, Berlin, Germany. All chemicals were used as received. The water used in all experiments was prepared in a three-stage Millipore Milli-Q Plus 185 purification system and had a resistivity higher than 18.2 MΩcm.

Methods. *Capsule and Multilayer Preparation*. A membrane filtration technique was employed to consecutively adsorb PSS and PDADMAC onto MF particles.[13] The adsorption of polyelectrolytes (1 mg/mL) was conducted in 0.5 M NaCl solution for 5 min. Three washings in H_2O followed. Then the respective oppositely charged polyelectrolyte species was adsorbed. After the desired number of layers was adsorbed, the coated particles were treated with HCl (pH 1.1) to decompose the MF cores. The produced MF oligomers and excess HCl were removed by filtration with gentle agitation until a neutral pH was established.

Multilayers of PSS/PDADMAC were assembled on mica by consecutively dip-coating the mica in polyelectrolyte solutions alternated with intermediate washings. The films were not dried before the next layer was adsorbed.

Capsule Annealing and Incubation in Salt Solution. Aqueous suspensions of capsules ($\sim 4 \times 10^8$ cm^{-3}) were incubated for 2 h at 40 °C. Salt-treated capsules were prepared by exposing them to 0.5 M NaCl at room temperature (23 °C) for 2 h. The

* Corresponding author. E-mail: edwin.donath@mpikg-golm.mpg.de.
† Zhejiang University.
‡ Max-Planck Institute of Colloids and Interfaces.
§ These authors contributed equally to this paper.

10.1021/jp000615i CCC: $19.00
Published on Web 07/12/2000

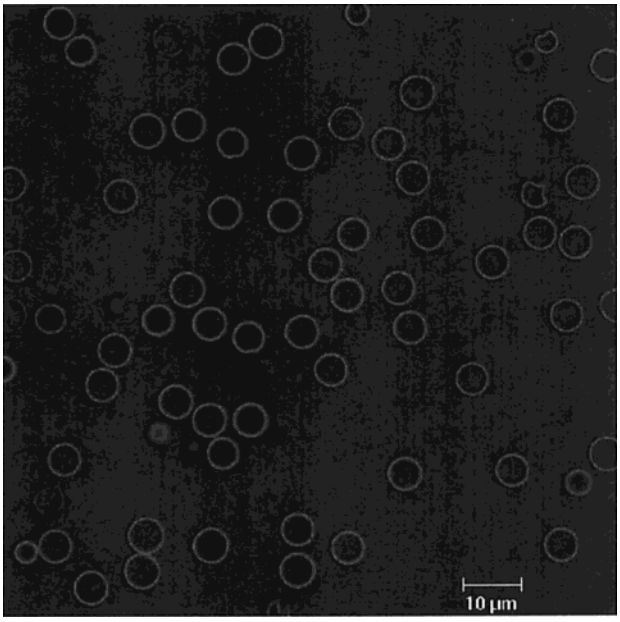

Figure 1. CLSM image of $(PSS/PDADMAC)_5$ capsules templated on MF particles of 3.8 μm diameter.

salt was then removed by centrifugation at 1145*g* (Sigma 3K30 Laboratory Centrifuges). Three washings in H_2O followed.

Scanning Force Microscopy (SFM). SFM images were recorded in air at room temperature (20−25 °C) using a Nanoscope III Multimode SFM (Digital Instrument Inc., Santa Barbara, CA). Silicon nitride (Si_3N_4) cantilevers with a force constant of 0.58 N/m (Digital Instrument) were used for contact SFM. Silicon tips (Olympus and Nanotips, DI) with a resonance frequency of ∼300 kHz and a spring constant of ∼40 N/m were employed for tapping mode SFM imaging. The contact force between the tip and the sample was kept as low as possible (<10 nN), and images were acquired in constant force mode (height mode) at a scan rate of 0.5−1 Hz. The samples were prepared by applying a drop of the capsule solution onto freshly cleaved mica or onto glass coverslips. Images were sampled from different areas. SFM images were processed by using Nanoscope software and Image PC software (Version beta 2, Scion Corp.). For the image analysis, a spatial autocorrelation function (ACF) was used.[14] It is defined as $g(\mathbf{r}_i-\mathbf{r}_j) = \langle I(\mathbf{r}_i)\text{-}I(\mathbf{r}_j)\rangle$, where $g(\mathbf{r}_i-\mathbf{r}_j)$ is the average (over all points of the image) of the product of the intensity (height) of a certain point at a position $\mathbf{r}_i$ and the intensity of another point at position $\mathbf{r}_j$. The function is therefore a measure of the mean size of areas of similar height, which, thus, represent either grains or the interstitials between them. The characteristic size of these areas is determined by the half-width at the half-height of $g(\mathbf{r}_i\text{-}\mathbf{r}_j)$. The existence of some lateral periodicity of the image height would result in oscillations of the autocorrelation function.

Confocal Laser Scanning Microscopy (CLSM). Confocal micrographs were taken with a Leica TCS NT confocal system (Leica, Germany) equipped with a 100×/1.4−0.7 oil immersion objective. For the observation of capsule sizes and shapes 6-carboxyfluorescein (6-CF) was used as a fluorescent label.

Rhodamine isothiocyanate labeled MF particles were used for following the core decomposition process by means of CLSM. A drop of the particle suspension was put onto a glass slide. After the water had evaporated, the focus was adjusted to the equatorial plane of the particles. Then a drop of HCl solution (pH 1.1) was applied. The core disintegration process was followed and a series of images as a function of time was taken using the "series scan" function of the equipment.

Results and Discussion

CLSM images showed that polyelectrolyte capsules consisting of five pairs of PSS/PDADMAC [$(PSS/PDADMAC)_5$] are continuous spherical films in aqueous solution (Figure 1). The capsule size was 5.5 ± 0.2 μm. This is remarkably larger than the dimensions of the template beeing 3.8 μm in diameter, since from single particle light scattering and from AFM we know that the wall thickness is below 20 nm. PSS/PAH capsules, however, always had a similar size as the template.

SFM investigations showed that in the dried state $(PSS/PDADMAC)_5$ polyelectrolyte capsules have collapsed as a result of evaporation of the aqueous content. The collapse of the capsule wall induced creases and folds (Figure 2a).

If one compares SFM images of PSS/PDADMAC capsules and PSS/PAH capsules it appears that the former seemed to have a rougher surface texture.[10] High-resolution SFM is a powerful method to inspect the capsule wall surface on the

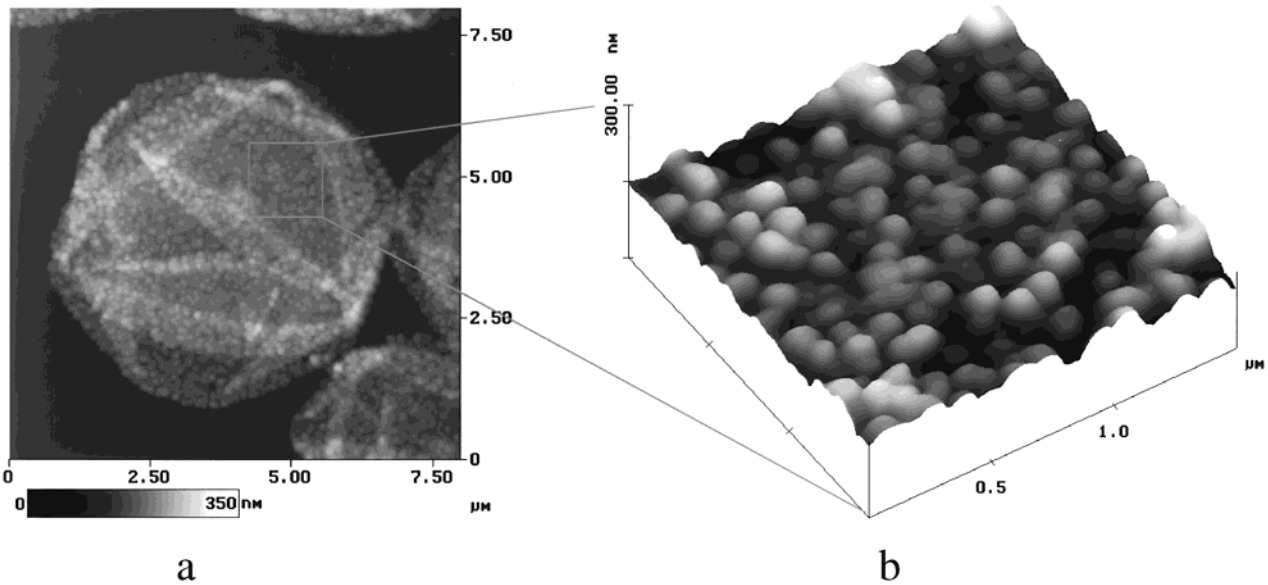

Figure 2. (a) SFM (contact mode) top-view image of a $(PSS/PDADMAC)_5$ capsule templated on MF particles of 3.8 μm diameter. (b) Three-dimensional SFM image (contact mode) of a part in part a as indicated by the box.

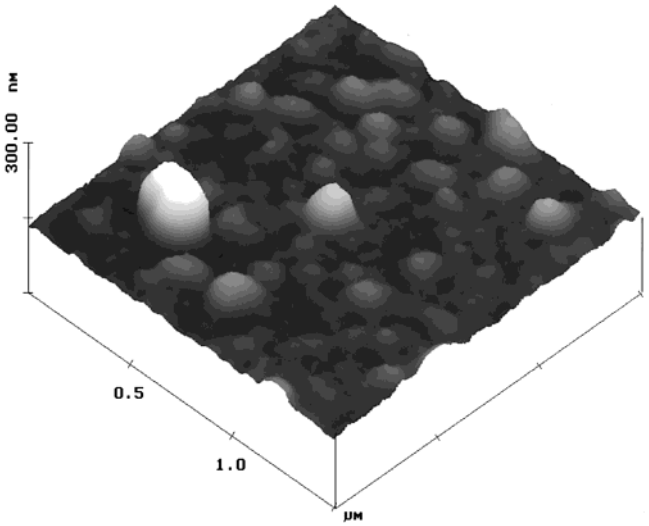

Figure 3. Three-dimensional SFM image (tapping mode) of (PSS/PDADMAC)$_5$ multilayers deposited on mica.

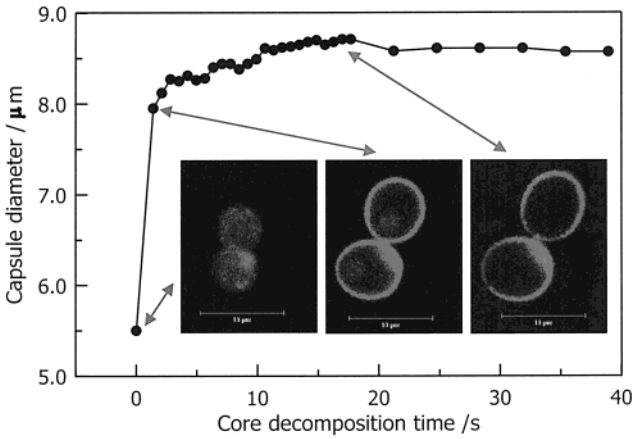

Figure 4. Diameter of (PSS/PDADMAC)$_5$ capsules templated on rhodamine-labeled MF particles of 5.5 μm as a function of core decomposition time in HCl (pH 1.1). The CLSM images in the inset correspond to the capsule sizes and treatment times as indicated by arrows.

nanometer scale. Therefore, further magnification of that part of the capsules that does not include any folds, as indicated in Figure 2a, is presented in Figure 2b. Indeed it shows that the surface texture of the collapsed capsule is quite rough. Grains are distributed homogeneously over the entire capsule surface. Interstitials between the grains can be clearly detected. Roughness (rms) calculations[14] over a 1.5 μm $\times$ 1.5 μm area free of folds provide a roughness measure perpendicular to the surface of $\sim$13 $\pm$ 0.5 nm, while a roughness of $\sim$10 $\pm$ 0.5 nm was found for PSS/PAH capsules.

By means of an autocorrelation analysis the lateral texture can be quantified in terms of an average lateral correlation length. From the high-resolution SFM images, such as shown in Figure 2b, the autocorrelation function is obtained. Fitting the curve into a Gaussian function and defining the half-width at half-height as the domain size, a lateral height correlation length of 124 $\pm$ 10 nm is obtained. Thus, this length is almost twice as big as for (PSS/PAH)$_5$ capsules, where the lateral correlation length was 70 $\pm$ 5 nm. Furthermore, the absence of a periodic pattern in the ACF confirms a random distribution of grains for PSS/PDADMAC capsules. The ACF texture analysis has the advantage that any arbitrary selection of a height threshold for defining a grain as in conventionally used grain analysis techniques is avoided.

A submicron lateral texture of layer-by-layer polyelectrolyte multilayers which were, however, self-assembled onto solid substrates has also been observed by other authors.[15−17] Kim et al.[16] have studied polyelectrolyte multilayers in dried state on gold and mica by SFM and reflection−absorption infrared (RAIR) spectroscopy. They conclude that randomly distributed polyelectrolyte grains of 80−100 nm in diameter are formed by adsorbed polyelectrolytes. We have suggested that these grains become visible as a result of drying.[10] Evaporation may have caused lateral segregation of the polymers due to the removal of water, which forms 50% of the polymer film volume prior to drying.[18] It was supposed that the grains reflect inherent inhomogeneities of the intermolecular polyelectrolytes interaction existing prior to drying.

In order to study the influence of the support, (PSS/PDADMAC)$_5$ multilayers were assembled on mica and inspected with SFM. The reconstructed 3-dimensional image is shown in Figure 3. A lateral grain structure of the multilayer surface is clearly observed. The grains are more inhomogeneously distributed compared with the free film (Figure 2b). Deep invaginations between the grains are not observed. The roughness of the supported film was $\sim$14 nm which is similar to that of the free film. A major contribution to this roughness comes from some larger inhomogeneities. Roughness calculation over an area apparently free of larger grains yielded a roughness of only $\sim$8−9 nm, demonstrating that the flat PSS/PDADMAC multilayer surface was smoother than a capsule surface apart from the presence of some large inhomogeneities. The lateral correlation length of 116 $\pm$ 12 nm is almost the same as for the PSS/PDADMAC capsules.

From the difference and similarities in the texture of the capsule walls and of the multilayers on mica, one can assume that the lateral organization of a multilayer and its roughness may not only depend on polyelectrolyte aggregation and subsequent segregation of these complexes caused by evaporation of water. It could also be that the greater freedom of movement in the free film compared with the substrate supported film has an influence on the roughness and lateral distribution. Capsule swelling upon core dissolution may also have affected the segregation of polyelectrolyte complexes. Therefore, the core dissolution process was studied in greater detail.

With CLSM it was observed that the PSS/PDADMAC capsules are larger than the templating cores. This was the result of capsule swelling occurring during the core dissolution process. The driving force for the swelling is the transient osmotic pressure difference created by the products of the core decomposition reaction. In this reduction the core material is depolymerized into smaller oligomers which can diffuse through the wall driven by concentration gradient and osmotic pressure. If the core decomposition is comparable or faster than permeation time of the products through the capsule walls, a concentration difference and, hence, a large osmotic pressure difference may build up.

Images of the swelling process together with the capsule diameter increase as a function of core decomposition time are shown in Figure 4. Within 2 s after acid addition, the capsules increased their size from 5.5 μm, the original core diameter, to approximately 8 μm and finally to about 8.7 μm at complete core removal which required about 20 s. Capsule swelling during the core decomposition process was also observed for PSS/PAH capsules. But the extent of swelling was much less. Continuous observations of PSS/PAH capsules, after core decomposition was apparently completed, show that these capsules shrink approximately to the template size. From these observations one

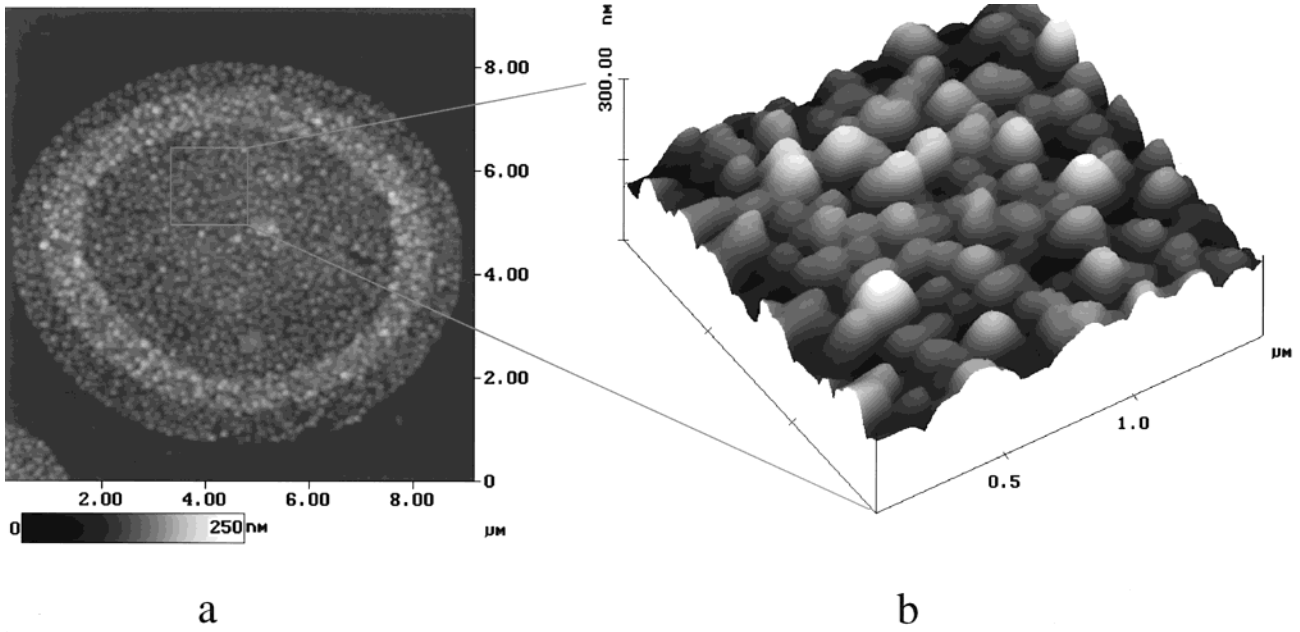

Figure 5. (a) SFM (contact mode) top-view image of a $(PSS/PDADMAC)_5$ capsule templated on MF particle of 3.8 μm diameter after incubation at 40 °C for 2 h in aqueous solution. (b) Three-dimensional SFM image (contact mode) of a part in part a as indicated by the box.

can conclude that the polyelectrolyte multilayer film of the PSS/PDADMAC capsule wall is stretched by a factor of 3 in area compared with the initial state just after deposition. This capability to stretch upon dissolution is a remarkable new feature of a free polyelectrolyte film not reported before. This area increase of the PSS/PDADMAC film cannot be explained by an elastic deformation since the area increase is permanent i.e., the change is plastic. (A detailed investigation of the swelling process revealed that, however, a small part of the area increase was transient.)

A possible influence of swelling on the texture of the PSS/PDADMAC capsule surface may be as follows. Initially existing inhomogeneities of the polyelectrolyte arrangement in the capsule multilayer are equivalent to inhomogeneities of the mechanical strength. Thicker parts of the multilayer are more resistant toward the lateral stress created by the osmotic pressure occurring during the core decomposition. Therefore, the multilayer may be inhomogeneously stretched. As a result of this process, preformed polyelectrolyte complexes are produced. The higher extent of capsule swelling in the core decomposition process compared with PSS/PAH capsules could facilitate the formation of the well-pronounced granular structure of the PSS/PDADMAC capsule wall observed by SFM in the dry state.

The composition of the multilayer is certainly responsible for its mechanical properties. Since PSS as the polyanion is the same in PSS/PAH and PSS/PDADMAC capsules, the observed difference in the osmotic response can be attributed to PDADMAC as the polycation and its specificity of interaction with PSS. A possible explanation would be that the interaction between PSS and PDADMAC is weaker than that with PSS and PAH. This permits a greater degree of layer stretching as a result of the applied osmotic pressure difference. This weaker interaction between PSS and PDADMAC can be explained by comparing the molecular architecture of PDADMAC with PAH. The average distance between monomers of PDADMAC is 0.375 nm,[19] which is larger than the length per monomer of PSS and PAH of 0.26 nm.[20] The distance of closest approach of the cationic and anionic charge in the PSS/PAH pair is 0.25 nm. Because of the presence of the methyl groups of the ammonium cations, the distance of the closest approach between the negative and positive charge in the PSS/PDADMAC pair is about 0.4 nm. Hence the mismatch of repeat distances between polycation and polyanion as well a higher distance of oppositely charged units together with a rather rigid PDADMAC is responsible for lower electrostatic interactions.

It can also be that the permeability of the core degradation products through a PSS/PDADMAC layer is smaller that that of a PSS/PAH layer. This would result in a greater osmotic stress for PSS/PDADMAC capsules, thus explaining their large degree of swelling. The fact that the roughness remained constant although the number of grains was reduced can be attributed to more pronounced interstitials caused by the increased segregation of grains.

In order to probe the strength of the interaction between PSS and PDADMAC and to see the influence on the lateral texture, the capsules were (i) subjected to a heat treatment and (ii) exposed to 0.5 M NaCl solution. After annealing for 2 h at 40 °C the PSS/PDADMAC capsules increased their size from 5.5 $\pm$ 0.2 to 7.5 $\pm$ 0.3 μm and the capsule wall thickness decreased from 22 $\pm$ 0.5 to 10 $\pm$ 0.5 nm, respectively. The grains were preserved after annealing as can be seen from Figure 5. The roughness of $\sim$13 nm has not significantly changed either. The control had a grain density of 64/μm^2, while the swollen capsules had only a density of 40/μm^2. Clearly, the domains are now further apart. The area had increased by a factor of $(7.5/5.5)^2 = 1.85 \pm 0.3$. The grain density decreased only by a factor of $64/40 = 1.6$. Thus, it can be concluded that within the error limits, the grain density decrease matched the area increase induced upon swelling.

When the capsules were exposed to 0.5 M NaCl, their size decreased together with a parallel increase of the wall thickness. The surface topology of the salt-exposed capsules at room temperature changed remarkably, as can be seen from the high-resolution SFM images in Figure 6. The grains can still be seen but are less well separated. Grains could be found in Figure 6. The roughness for the salt-exposed capsules was 16 nm. The lateral correlation length calculated by ACF was increased by almost a factor of 2 to 291 $\pm$ 42 nm. This can be explained by a diminished segregation of the previously well separated

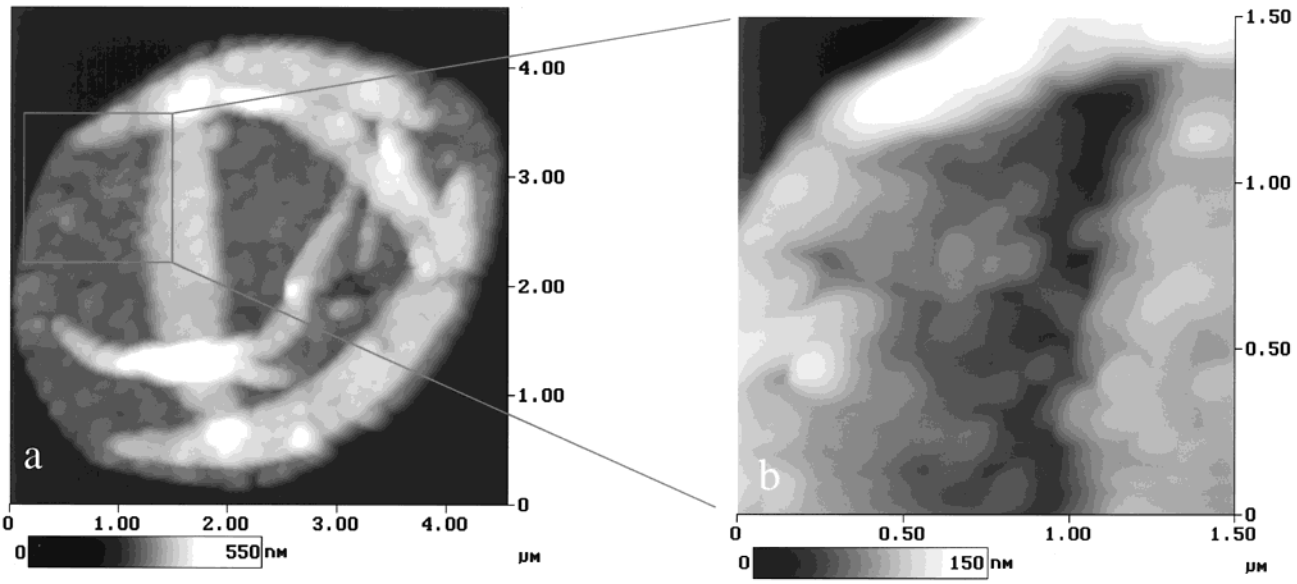

Figure 6. (a) SFM (contact mode) top-view image of a $(PSS/PDADMAC)_5$ capsule templated on MF particle of 3.8 μm diameter incubated in 0.5 M NaCl at room temperature for 2 h. (b) SFM top-view image of a part in part a as indicated by the box.

polyelectrolyte domains induced by capsule shrinking as a result of the treatment with salt.

Let us compare lateral correlation length which is a measure of the grain size with the volume occupied by a stoichiometric complex of PDADMAC/PSS. The molecular weight of PDADMAC was 220 000−350 000, which is equivalent to approximately 1500−2500 monomers per chain. If one assumes an average monomer number per chain of 2000, this would give a contour length of 700 nm. Such a chain occupies a volume of about 700 nm^3.[19] Taking into account that exactly 700 monomers of similar size of PSS would bind to the PDADMAC molecule under consideration and that 50% of the layer are occupied by H_2O, the volume of a stoichiometric PDADMAC/PSS complex should be approximately 2800 nm^3. A disk occupying 2800 nm^3 with a height of 2 nm (the layer thickness increment) would have a diameter of 42 nm. This number is only 3 times smaller than the measured domain size of 124 ± 10 nm. Thus, $3^2 = 9$ stoichiometric complexes would constitute such a grain of 120 nm in diameter. Since a statistically formed cationic−anionic polyelectrolyte complex represents a network of polyelectrolyte molecules, it is quite conceivable that the observed grains represent some average of more closely connected individual polymers.

Concluding Remarks

In summary, one can conclude that the grains observed with SFM represent complexes of several polyelectrolyte molecules. Their size and distribution depend on the layer material and the layer stretching. The swelling of the capsules during the core decomposition produced a segregation of the grains, because the area increase is not homogeneous. A relatively larger area increase takes place between the grains. It can be further concluded that the electrostatic interaction between the polymers influences the texture of the capsule wall, since an incubation of the capsules with salt solution induced a capsule size decrease and a wall thickness increase, correspondingly. Heating in water, however, leads to area increase and subsequently to a progressing segregation of the grains. The nature of the heating induced area increase in water is at present not well understood. It may be a result of the tendency of the polyelectrolytes to stretch if the counterion screening becomes insufficient. It has to be remembered that the polyelectrolytes were assembled in 0.5 M NaCl. A direct demonstration that drying was essential for the formation of grain structure is currently difficult to obtain.

A remarkable advantage of polyelectrolyte capsules is their potential variability in composition. A variety of substances can be incorporated as layer constituents. For example, lipids and nanoparticles can be used as layer materials.[11,21,22] It is a challenging task to explore the layer properties, such as their morphology, mechanics, and transport features as a function of their composition and method of fabrication. Having realized and understood that the nanostructure strongly depends on molecular and enviromental parameters, we also have means to tailor macroscopic properties. As was shown in this study, SFM is a powerful technique for characterizing the texture of the capsule surface. Further work to explore the annealing and salt effects in greater detail and studies relating the permeability and elasticity to the composition and the structure of the capsule walls is currently underway.[9]

Acknowledgment. We thank Dr. K.-H. Lerche, Microparticles GmbH, Berlin, Germany, for the supply of monodisperse soluble MF particles. C.G. thanks the DAAD and the Max Planck Society for the financial support. The work was partially supported by a grant from BMBF No. 03C0293A1.

References and Notes

(1) Decher, G. *Science* **1997**, *277*, 1232.

(2) Decher, G. In *Templating, Self-Assembly and Self-Organisation*; Sauvage, J.−P., Hosseini, M. W., Eds.; Pergamon: Oxford, UK, 1996; Vol. 9, p 507.

(3) Decher, G.; Hong, J. D.; Schmitt, J. *Thin Solid Films* **1992**, *210/211*, 831.

(4) Keller, S. W.; Johnson, S. A.; Brigham, E. S.; Yonemoto, E. H.; Mallouck, T. E. *J. Am. Chem. Soc.* **1995**, *117*, 12879.

(5) Donath, E.; Sukhorukov, G.; Caruso, F.; Davis, S.; Möhwald, H. *Angew. Chem., Int. Ed.* **1998**, *37*, 2201.

(6) Sukhorukov, G. B.; Brumen, M.; Donath, E.; Möhwald, H. *J. Phys. Chem. B* **1999**, *31*, 6434.

(7) Sukhorukov, G. B.; Donath, E.; Lichtenfeld, H.; Knippel, E.; Knippel, M.; Budde, A.; Möhwald, H. *Colloids Surf. A* **1998**, *137*, 253.

(8) Sukhorukov, G.; Donath, E.; Davis, S.; Lichtenfeld, H.; Caruso, F.; Popov, V.; Möhwald, H. *Polym. Adv. Technol.* **1998**, *9*, 759.

(9) Leporatti, S.; Gao, C.; Voigt, A.; Donath, E.; Möhwald, H. *Eur. Phys. J. E.*, submitted for publication.

(10) Leporatti, S.; Voigt, A.; Mitlöhner, R.; Sukhorukov, G.; Donath, E.; Möhwald, H. *Langmuir* **2000**, *16*, 4059.

(11) Moya, S.; Sukhorukov, G. B.; Auch, M.; Donath, E.; Möhwald, H. *J. Colloid Interface Sci.* **1999**, *216*, 297.

(12) Georgieva, R.; Moya, S.; Reichle, C.; Leporatti, S.; Neu, B.; Bäumler, H.; Donath, E.; Möhwald, H. *Langmuir*, in press.

(13) Voigt, A.; Lichtenfeld, H.; Sukhorukov, G. B.; Zastrow, H.; Donath, E.; Bäumler, H.; Möhwald, H. *Ind. Eng. Chem. Res.* **1999**, *38*, 4037.

(14) Gheber, L. A.; Edidin, M. *Biophys. J.* **2000**, *77*, 3163. Nanoscope Software, Digital Instruments.

(15) Lvov, Y.; Onda, M.; Ariga, K.; Kunitake, T. *J. Biomater. Sci. Polymer. Ed.* **1998** *9*, 4, 345.

(16) Kim, D.; Han, S. W.; Kim, C. H.; Hong, J. D.; Kim, K. *Thin Solid Films* **1999**, *350*, 153.

(17) Lvov, Y.; Ariga, K.; Onda, M.; Ichinose, I.; Kunitake, T. *Colloids. Surf. A* **1999**, *146*, 337.

(18) Ruths, J.; Essler, F.; Decher, G.; Riegler, H. *Langmuir*, in press.

(19) de Meijere, K.; Netz, R.; Joanny, J.−F.; Donath, E.; Brezesinski, G.; Möhwald, H., submitted to *Proc. Natl. Acad. Sci. USA.*

(20) Donath, E.; Walther, D.; Shilov, V. N.; Knippel, E.; Budde, A.; Lowack, K.; Helm, C. A.; Möhwald, H. *Langmuir* **1997**, *13*, 20, 5294.

(21) Sukhorukov, G. B.; Donath, E.; Moya, S.; Susha, A. S.; Voigt, A.; Hartmann, J.; Möhwald, H. *J. Microencapsulation* **2000**, *17* (2), 177.

(22) Caruso, F.; Caruso, R. A.; Möhwald, H. *Science* **1998**, *6 Nov*, 282, 1111.